Understanding the impacts of catchment characteristics on the shape of the storage capacity curve and its influence on flood flows

Hongkai Gao, Huayang Cai and Zheng Duan

ABSTRACT

In various conceptual models, the shape parameter (β) of the storage capacity curve, representing the non-linear relationship between relative soil moisture and runoff, determines runoff yield given certain circumstances of rainfall and antecedent soil moisture. In practice, β is typically calibrated for individual catchments and for different purposes, which limits more systematic understanding and also prediction in ungauged basins. Moreover, its regionalization and linkage to catchment characteristics is also not well understood, especially in relation to large-sample datasets. In this study, we used 404 catchments in the USA to explore β regionalization and attributes in relation to key catchment characteristics: elevation, slope, depth-to-bedrock, soil erodibility, forest cover, urban area, aridity index, catchment area, and stream density. We found a clear regionalized pattern of β, coherent with topography. Comparisons between β and various features demonstrated that slope has the largest impact. Land-cover, soil, geology, and climate also have an impact, but with lower correlation coefficients. This finding not only reveals spatial variation in β, but also deepens our understanding of its linkage to catchment features and flood flows. Moreover, the results provide a useful reference for decision-makers for flood prevention and mitigation.

Key words | catchment characteristics, FLEX model, flooding, MOPEX, peak flow, storage capacity curve

Hongkai Gao
Guangdong Engineering Technology Research Center of Water Security Regulation and Control for Southern China,
Sun Yat-sen University,
Guangzhou 510275,
China
and
Julie Ann Wrigley Global Institute of Sustainability,
Arizona State University,
Tempe,
AZ 85287,
USA

Huayang Cai
Institute of Estuarine and Coastal Research, School of Marine Sciences,
Sun Yat-sen University,
Guangzhou 510275,
China

Zheng Duan (corresponding author)
Chair of Hydrology and River Basin Management,
Technical University of Munich,
Arcisstrasse 21,
80333 Munich,
Germany
E-mail: *duanzheng2008@gmail.com*; *zheng.duan@tum.de*

INTRODUCTION

Flooding is one of the leading natural hazards (Hirabayashi *et al.* 2013; Blaikie *et al.* 2014; Winsemius *et al.* 2016), causing significant casualties and property damage globally every year (DHI 2012; Blaikie *et al.* 2014). Flood peak flow is one of the most important variables in flood modelling and forecasting. The impacts of rainfall amount, intensity and the antecedent soil moisture on flood generation have been well studied (Yu *et al.* 1999, 2000; Blöschl *et al.* 2015; Berghuijs *et al.* 2016). However, the impact of catchment features on flood peak flow is neither systematically studied nor well explored, particularly in large-sample datasets. This lack of understanding hinders improved understanding of catchment storm-flood processes, and furthermore, prediction in ungauged basins (Sivapalan *et al.* 2003).

Additionally, understanding the mechanisms of storm-flood processes and their link to catchment features is essential for decision-making on flood prevention and mitigation (Palmer *et al.* 2015), as well as land-use planning (Andréassian 2004; Sriwongsitanon & Taesombat 2011). Understanding relationships between flood flows and catchment features is also beneficial for prediction of future hydrological changes (Xu & Singh 2004; Xu *et al.* 2005; Milly *et al.* 2008; Montanari *et al.* 2013), and the impact of land use changes (Stonestrom *et al.* 2009). Therefore, there

doi: 10.2166/nh.2017.245

is an urgent need to improve our understanding of linkages between floods and catchment characteristics.

Partitioning rainfall into runoff and infiltration is the central question of all hydrological models (Singh & Woolhiser 2002; Beven 2012). It also plays an important role in land surface modelling (Sellers *et al.* 1996; Dai *et al.* 2003) and biogeochemical modelling studies (Austin *et al.* 2004) due to the fact that energy and nutrients are transported with the movement of water (Mo & Zhang 2013). The dominant perceptual models (Beven 2012) of rainfall-runoff process mechanisms are infiltration excess overland flow (Hortonian overland flow (HOF)) (Horton 1933), and saturation excess flow (SEF) (Hewlett 1961; Dunne & Black 1970). HOF, in conjunction with the unit hydrograph, dominated engineering hydrology for several decades in the early 20th century (Beven 2004a). However, findings from more and more field experiments (Sklash & Farvolden 1979; Beven 2004b; Burt & McDonnell 2015) questioned the role of HOF, even in arid catchments (Liu *et al.* 2012; Li *et al.* 2014). In contrast, the SEF theory, also known as the variable contributing area (VCA) model, assumes that only certain saturated areas of the catchment, contribute to runoff yield (Hewlett 1961; Dunne & Black 1970; Hewlett & Troendle 1975). The saturated area varies with different soil moisture conditions, and is strongly impacted by the spatial heterogeneity of the storage capacity at a catchment scale. This theory has been implemented in various conceptual hydrological models, i.e. Xinanjiang (Zhao *et al.* 1980), HBV (Bergström & Forsman 1973; Bergström & Lindström 2015), TOPMODEL (Beven & Kirkby 1979), GR4 J (Perrin *et al.* 2001). All these models have demonstrated good performance in streamflow simulation in many catchments (Singh & Woolhiser 2002). The Xinanjiang, HBV and GR4 J models apply a conceptual storage-contributing area relationship to estimate the event runoff yield. The TOPMODEL assumes that topography determines the relation of storage-contributing area, and Dynamic Topmodel improves this idea by including landscape information (Beven & Freer 2001).

The amount of rainfall and the antecedent soil moisture are two essential variables to determining the amount of runoff in SEF-type conceptual models. However, it should be noted that different catchments will likely generate different amounts of runoff even with the same amount of rainfall and precedent soil moisture, due to the different spatial distribution of unsaturated storage, which is controlled by land surface features. Many efforts have been made to study the impacts of extreme precipitation events and antecedent soil moisture on flood peak flows (Blöschl *et al.* 2015; Berghuijs *et al.* 2016), however, very few studies have systematically explored the influence of various catchment land surface features (except for land cover, see Andréassian 2004; Blöschl *et al.* 2007) on flood flows. In conceptual hydrological models, such as Xinanjiang, HBV, and GR4 J, catchment features are expressed by two essential parameters: the root zone storage capacity (S_{uMax}) and the shape of the storage capacity curve (often termed β). The former was found to be controlled by climate (Gao *et al.* 2014a), and determines the long-term runoff coefficient and evaporation. The latter reflects the spatial distribution of the storage capacity (Zhao 1992; Sivapalan & Woods 1995), and determines the peak flow given the amount of rainfall and antecedent soil moisture. As a result, the shape of the storage capacity curve is useful in estimating the amount of runoff yield and more importantly, the flood peak flow. Further details about the shape of the root zone storage capacity curve β are given below in Methodology: Storage capacity curve and flood.

Parameter regionalization is an approach to understanding the spatial distribution of parameters (Merz & Blöschl 2004; Kling & Gupta 2009) and the correlations between optimized parameter values and catchment physical features (Samaniego *et al.* 2010). Undertaking parameter regionalization is not only beneficial for understanding the linkages between parameters and catchment features, but also helpful in predicting hydrological processes in ungauged basins (Hrachowitz *et al.* 2013). However important questions remain. For example, the β parameter was hypothesized to be determined by topography and geology (Zhao *et al.* 1980), but Sivapalan & Woods (1995) found that soil depth distribution also plays a determinative role in β estimation. Therefore, further studies are required to explore the spatial distribution pattern of β, and its linkage to the physical features of catchments.

The representativeness and comprehensiveness of sample data used for hypothesis testing is an important point to consider in hydrological studies considering the uniqueness of different catchments. Since findings from a

limited number of catchments may be only applicable at local and regional scales, wider generalization to other catchments may be problematic. Large sample data sets are therefore essential for hypothesis testing and the drawing of robust conclusions for diverse environments (Gupta *et al.* 2014). Additionally, the knowledge gained from regional studies needs to be confirmed and validated by sufficiently large sample datasets due to the complexity of catchment characteristics. Moreover, over the past decades, great efforts have been made to collate and share hydrological data sets, leading to increasing availability of relevant data sets for a large number of catchments at continental and global scales, thereby facilitating large-sample empirical studies. These hydrological datasets include, for example, MOPEX (Model Parameter Estimation Experiment) for the contiguous United States (CONUS) (www.nws.noaa.gov/oh/mopex/), the datasets of the UK (https://nrfa.ceh.ac.uk/), France (www.cnrm.meteo.fr/isbadoc/projects/rhoneagg/), and Australia (Peel *et al.* 2000). In addition, global datasets include GEWEX (www.gewex.org/) and GLACE (gmao.gsfc.nasa.gov/research/GLACE-2/). The MOPEX data (Duan *et al.* 2006) contain good quality daily data of key variables for 438 catchments in the USA, and will be used in this study.

In this study, the Xinanjiang storage capacity curve (Zhao *et al.* 1980; Liang *et al.* 1994), widely used in hydrological and land surface modelling, was coupled with the FLEX model framework (Fenicia *et al.* 2011; Gao *et al.* 2014b; Gharari *et al.* 2014). This approach was applied to simulate the hydrological processes of the large-sample MOPEX catchments, and to calibrate the β parameter which determines the flood peak flow given certain soil moisture conditions. Subsequently, correlations between β and typical catchment characteristics were explored. These included topography, soil hydraulic characteristics, climate, vegetation cover, urban area, geology (soil depth to bedrock), basin area and area of impermeable surfaces. We aimed at answering the following three questions in this study: (1) Is there any regionalized pattern of the parameter of the shape of storage capacity curve (β)? (2) Which catchment characteristics affect the β value and the catchment peak flows, and to what extent? (3) What is the physical meaning behind the linkages between the β value and catchment characteristics?

DATASETS

MOPEX dataset and general approach

The MOPEX data were collated for hydrological model parameter estimation experiments (Duan *et al.* 2006), and contain relevant data for 438 catchments in the USA, including, daily precipitation, daily maximum and minimum air temperature, and daily streamflow from 1948 to 2003. Thirty-four catchments with short streamflow observations (less than 3 years of continuous streamflow data) were excluded, while the remaining 404 catchments were used in this study. Among these catchments, rainfall-runoff flooding is the dominant flood/runoff generation mechanism, but snowmelt-runoff flooding also occurs (Berghuijs *et al.* 2016). Temperature data were used to estimate snowmelt and its potential evaporation. Precipitation and calculated potential evaporation are the two major input forcings for the rainfall-runoff model. Daily streamflow was used to calibrate the free parameters in the hydrological model. Further details of the modelling process are given later in section Methodology: Storage capacity curve and flood.

Landscape datasets

Various types of landscape information have been collated and further details are provided below and in Table 1.

Topography

The digital elevation model (DEM) of the CONUS at 90 m resolution (Figure 1) was downloaded from the Earth Explorer of United States Geological Survey (USGS, http://earthexplorer.usgs.gov/). Slope (in degrees) (Figure 1) was derived from the DEM using ArcMap toolbox. For each catchment, the average elevation and slope values were calculated and used to represent the catchment elevation and slope for further analysis.

Geology

Depth to bedrock was regarded as the integrated geologic indicator for hydrological processes, since bedrock as the

Table 1 | Datasets used in this study

Data	Unit	Resources	Website	Reference
Daily precipitation	mm/d	MOPEX	http://www.nws.noaa.gov/ohd/mopex/mo_datasets.htm	Duan *et al.* (2006)
Daily maximum temperature	°C	MOPEX	Same as above	Same as above
Daily minimum temperature	°C	MOPEX	Same as above	Same as above
Daily dupli	mm/d	MOPEX	Same as above	Same as above
Area	km^2	MOPEX	Same as above	Same as above
Aridity index	–	MOPEX	Same as above	Same as above
DEM	m	USGS	http://earthexplorer.usgs.gov/	–
Slope	degrees	USGS	Same as above	–
Depth to bedrock	cm	STATSGO	http://www.soilinfo.psu.edu/index.cgi?soil_data&conus&data_cov&dtb	Schwarz & Alexander (1995)
K factor of soil	–	USGS	http://water.usgs.gov/GIS/metadata/usgswrd/XML/muid.xml	Wolock (1997)
Percentage of urban	%	NLCD	http://www.mrlc.gov/	Homer *et al.* (2015)
Percentage of forest cover	%	NLCD	http://www.mrlc.gov/	Homer *et al.* (2015)
Stream density	km/km^2	Horizon Systems Corporation	http://www.horizon-systems.com/nhdplus/	–

lower boundary of subsurface stormflow substantially impacts the saturated storage capacity and then runoff generation processes and flooding (Tromp-van Meerveld & McDonnell 2006). The depth to bedrock data (Schwarz & Alexander 1995) (Figure 1) were accessed from STATSGO (State Soil Geographic, http://www.soilinfo.psu.edu/index.cgi?soil_data&conus&data_cov&dtb). The average depth to bedrock for each catchment was calculated by ArcGIS toolbox and used for further analysis.

Soil

Soil texture is synthetically represented by the K factor, since the K factor is a lumped soil erodibility factor which represents the soil profile reaction to soil detachment caused by raindrops and surface flow (Renard *et al.* 2011). Generally, the soils (high in clay and sand) have low K values, and soils with high silt content have larger K values. The K factor for each catchment was calculated from soil survey information available from USGS (Wolock 1997).

Land use

Land use data were obtained from National Land Cover Database (NLCD, http://www.mrlc.gov/nlcd.php). Due to the complexity of land use information, we selected the proportion of forest cover and the urban area proportion (Figure 1) as two integrating indicators to distinguish the driving force either by nature or human impacts. Forest plays an essential role in hydrological processes (Jasechko *et al.* 2013), especially in the runoff generation processes (Brooks *et al.* 2010). The proportion of urban area is a proxy land use change related to human activities (Grimm *et al.* 2008), with consequent impacts on catchment hydrology (Lee & Heaney 2003).

Catchment area and stream density

Area data were obtained from the MOPEX dataset. Stream density (km/km^2) is the total length of all the streams and rivers in a drainage basin divided by the total area of the drainage basin. Stream density was obtained from Horizon Systems Corporation (Table 1).

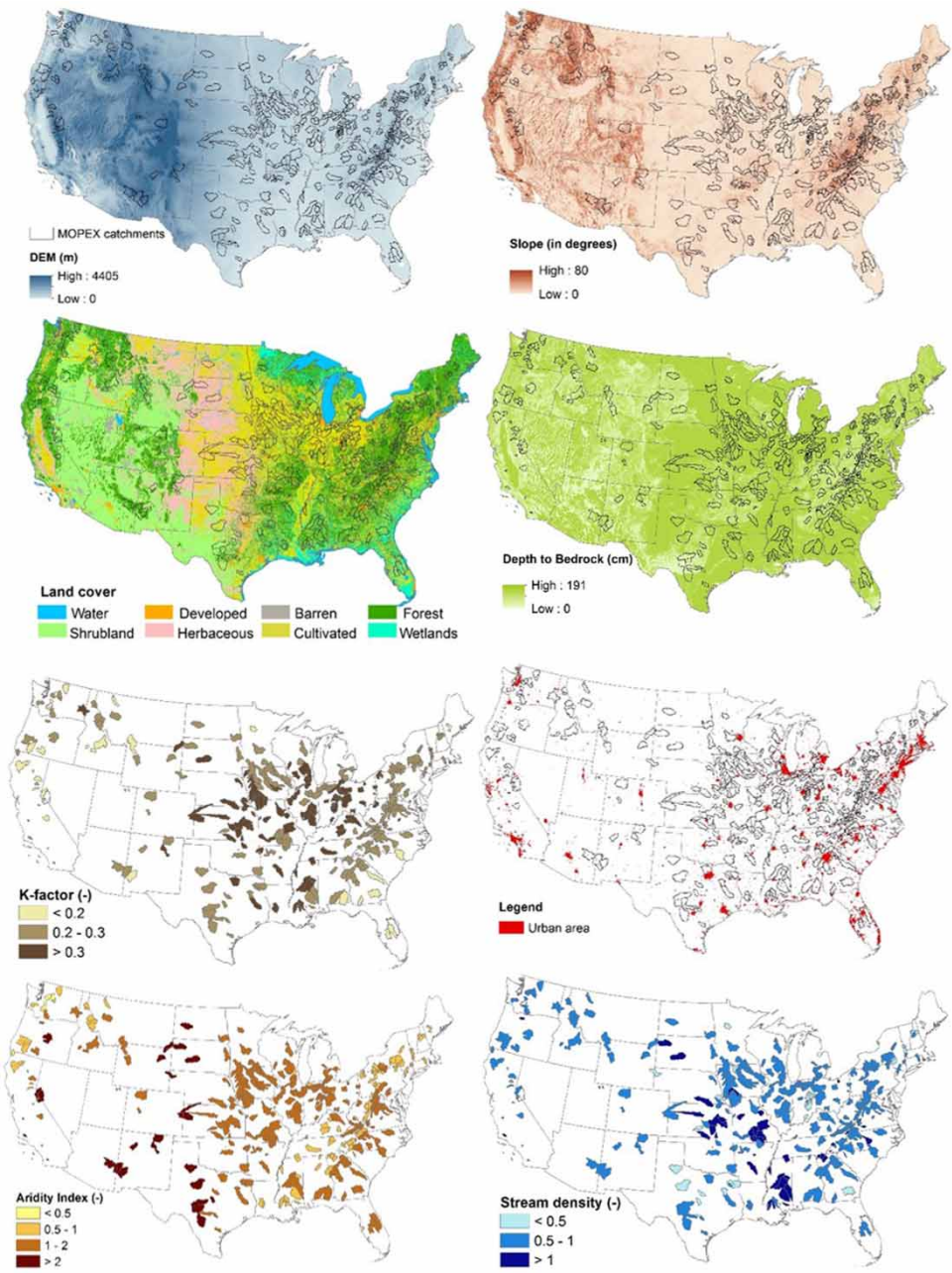

Figure 1 | Maps of the DEM, slope (in degrees), land cover, depth to bedrock, K-factor of soil, urban area, aridity index, and stream density of the CONUS, with the boundaries of 404 MOPEX catchments.

Climate

Daily potential evaporation was estimated using the Hargreaves equation with maximum and minimum daily temperature from MOPEX as input (Hargreaves & Samani 1985). The aridity index (long term potential evaporation divided by long term precipitation) was selected to represent the climate for a given catchment (Budyko 1974; Fu 1981), and long-term mean annual precipitation and estimated potential evaporation from MOPEX datasets was used to compute the aridity index for individual catchments.

METHODOLOGY

FLEX model structure

We used the FLEX modelling framework to simulate the hydrological processes of the MOPEX catchments in this study. The FLEX framework permits flexibility in model structures for different modelling purposes (Fenicia *et al.* 2008; Gao *et al.* 2014b; Gharari *et al.* 2014). For example, the snowmelt and interception processes have been included in this study for relevant MOPEX catchments. The FLEX framework has been used successfully to simulate streamflow in diverse catchments, with satisfactory performance (Fenicia *et al.* 2008; Gao *et al.* 2014b; Gharari *et al.* 2014; Li *et al.* 2014; Zhao *et al.* 2016).

The FLEX model contains five conceptualized reservoirs, including the snow reservoir (S_w), interception reservoir (S_i), unsaturated reservoir (S_u), and the two recession reservoirs (S_f and S_s). Snowmelt was calculated by a widely used parsimonious temperature-index method (Hock 2003; Gao *et al.* 2012, 2017). Before infiltration occurs, precipitation/snowmelt is first intercepted by the vegetation canopy. In this study, the interception was estimated by a threshold parameter (I_{max}), below which all precipitation was intercepted and evaporated (De Groen & Savenije 2006). The effective rainfall/snowmelt is split by the Xinanjiang storage capacity curve (further details are given in the next section), into generated runoff (R_u) and infiltration. The generated runoff (R_u) is further split into two fluxes, the flux to the fast response reservoir (R_f) and the flux to the slow response reservoir (R_s), by a splitter (D). The delayed time from storm to the flood peak is estimated by a convolution delay function, with a time delay of T_{lagF}. Subsequently, the fluxes into two different response reservoirs (S_f and S_s) is controlled by two linear equations between discharge and storage, representing the subsurface storm flow and the groundwater flow, respectively. The two discharges (Q_f and Q_s) were merged to generate the simulated streamflow (Q_m). The model parameters are shown in Table 2, while the equations are given in Table 3. A more detailed description of the model structure can be found in Gao *et al.* (2014b). The FLEX model has a total of 10 free parameters to be calibrated that are shown in red in Figure 2.

Table 2 | The parameters of FLEX model, and their prior ranges for calibration

Parameter	Explanation	Prior range for calibration
F_{DD} (mm/(d °C^{-1}))	Degree-day factor	(1, 10)
T_t (°C)	Threshold temperature	(−2, 6)
I_{max} (mm)	Maximum interception capacity	(0.1, 6)
S_{uMax} (mm)	The root zone storage capacity	(10, 1,000)
β (−)	The shape of the storage capacity curve	(0.01, 5)
C_e (−)	Soil moisture threshold for reduction of evaporation	(0.1, 1)
D (−)	Splitter to fast and slow response reservoirs	(0, 1)
T_{lagF} (d)	Lag time from rainfall to peak flow	(0, 10)
K_f (d)	The fast recession coefficient	(1, 20)
K_s (d)	The slow recession coefficient	(20, 400)

In Figure 2, precipitation (P) is split into snowfall (P_s) and rainfall (P_f) based on threshold temperature (T_t). Snowmelt is calculated based on the temperature-index method, using degree-day factor (F_{DD}). Rainfall is intercepted by an interception reservoir (S_i) with a capacity parameter I_{max} (mm). P_e (mm d^{-1}) is the effective rainfall to soil surface. The unsaturated reservoir (S_u) is used to split the P_e (mm d^{-1}) into generated runoff R_u (mm d^{-1}) and infiltration by two free parameters S_{uMax} (mm) and β (−). C_e (−) controls the relationship between soil moisture and actual evaporation. R_u recharges two linear reservoirs (S_f and S_s) by a parameter (D) and delay time parameter (T_{lagF}). The response processes of subsurface storm flow Q_f (mm d^{-1}) and groundwater runoff Q_s (mm d^{-1}) are modelled with two recession parameters, K_f (d) and K_s (d).

Storage capacity curve and flood

The Xinanjiang storage capacity curve applied in the FLEX model was used to calculate the runoff generation

Table 3 | The water balance and constitutive equations used in FLEX model (Gao *et al.* 2014b)

Reservoirs	Water balance equations	Constitutive equations
Snow reservoir	$\frac{dS_w}{dt} = P_s + R_{rf} - M_s$ (1)	$M_s = \begin{cases} F_{dd}(T - T_t); & T > T_t \\ 0; & T \le T_t \end{cases}$ (2)
Interception reservoir	$\frac{dS_i}{dt} = P_r - E_i - P_{tf}$ (3)	$E_i = \begin{cases} E_p; S_i > 0 \\ 0; S_i = 0 \end{cases}$ (4)
		$P_{tf} = \begin{cases} 0; S_i < I_{max} \\ P_r; S_i = I_{max} \end{cases}$ (5)
Unsaturated reservoir	$\frac{dS_u}{dt} = P_e - E_a - R_u$ (6)	$\frac{R_u}{P_e} = 1 - \left(1 - \frac{S_u}{(1+\beta)S_{uMax}}\right)^{\beta}$ (7)
		$\frac{E_a}{E_p - E_i} = \frac{S_u}{C_e S_{uMax}}$ (8)
Splitter and Lag function		$R_f = R_u D$ (9)
		$R_s = R_u(1 - D)$ (10)
		$R_{fl}(t) = \sum_{i=1}^{T_{lagf}} c_f(i) \cdot R_f(t - i + 1)$ (11)
		$c_f(i) = \frac{i}{\sum_{u=1}^{T_{lagf}} u}$ (12)
		$R_{sl}(t) = \sum_{i=1}^{T_{lags}} c_s(i) \cdot R_s(t - i + 1)$ (13)
		$c_s(i) = \frac{i}{\sum_{u=1}^{T_{lags}} u}$ (14)
Fast reservoir	$\frac{dS_f}{dt} = R_f - Q_f$ (15)	$Q_f = \frac{S_f}{K_f}$ (16)
Slow reservoir	$\frac{dS_s}{dt} = R_s - Q_s$ (17)	$Q_s = \frac{S_s}{K_s}$ (18)

from S_u and investigate the impact of catchment features on the curve parameter (β) and the flood volumes and peaks. The Xinanjiang storage capacity curve has been widely used in various hydrological and land surface models, e.g. the Variable Infiltration Capacity (VIC) model (Liang *et al.* 1994), the ARNO model (Todini 1996), the Probability Distributed Model (PDM) model (Moore 2007), and SUPERFLEX (Fenicia *et al.* 2011). The function for the storage capacity curve (see also Equation (7)), is written as:

$$\frac{f}{F} = 1 - \left(1 - \frac{S_u}{(1+\beta)S_{uMax}}\right)^{\beta} \quad (19)$$

where f (L^2) indicates the saturated/contributing area, and F (L^2) is the entire catchment area, f/F (–) is the fraction of saturated contributing area, and S_u (mm) indicates soil moisture. There are two parameters (S_{uMax} and β) in the

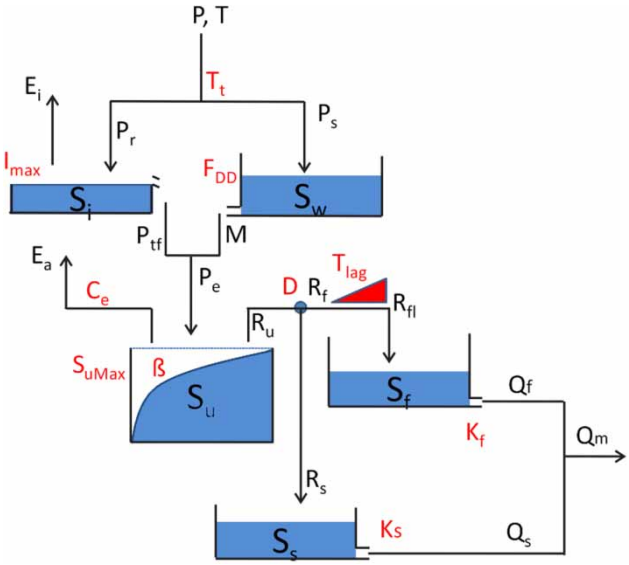

Figure 2 | The FLEX hydrological model structure. Red symbols indicate parameters, and black indicate storage components and fluxes. Please refer to the online version of this paper to see this figure in colour: http://dx.doi.org.10.2166/nh.2017.245.

function for the storage capacity curve. It is worth noting that different definitions of S_{uMax} (mm) are used in the literature (Zhao *et al.* 1980; Liang *et al.* 1994; Sivapalan & Woods 1995; Moore 2007; Gao *et al.* 2014a). In this study, we define S_{uMax} as the catchment averaged root zone storage capacity (Gao *et al.* 2014a), since the root zone is the critical layer in soil that determines catchment water balance, i.e. the evaporation, transpiration and runoff generation; while β determines the spatial distribution pattern of S_{uMax} in a catchment. Runoff is estimated based on the relative soil moisture (S_u/S_{uMax}), and the shape of the curve determined by β.

Different shapes of the curve will generate different amounts of runoff under the same rainfall and antecedent soil moisture conditions (Zhao *et al.* 1980). The prior range of β is recommended to be between 0.1 and 0.4 by the original model developer (Zhao *et al.* 1980). However, Liang *et al.* (1994) found that the optimized β can be 0.001 in certain catchments, while Wood *et al.* (1992) found that the optimized β could be larger than 1 in some cases. Sivapalan & Woods (1995) recommended setting the prior range as 0.01 to 5.

In order to illustrate the impact of varying β on the storage capacity curve and runoff generation, we conducted a scenario analysis (Figure 3) using the following assumptions: $S_{uMax} = 100$ mm, antecedent soil moisture (S_u) = 50 mm, instantaneous precipitation is set as 20 mm, and all initial conditions and other relevant parameters are kept the same. If $\beta = 0$, the storage capacity curve becomes a simple rectangular bucket, and no runoff will be generated until the rectangular bucket is full. Therefore, there is no runoff yield in this case because the rectangular bucket is not saturated, even after 20 mm rainfall. If β is larger than 0 and less than 1, the storage capacity curve will be a convex curve, which indicates that most runoff will be

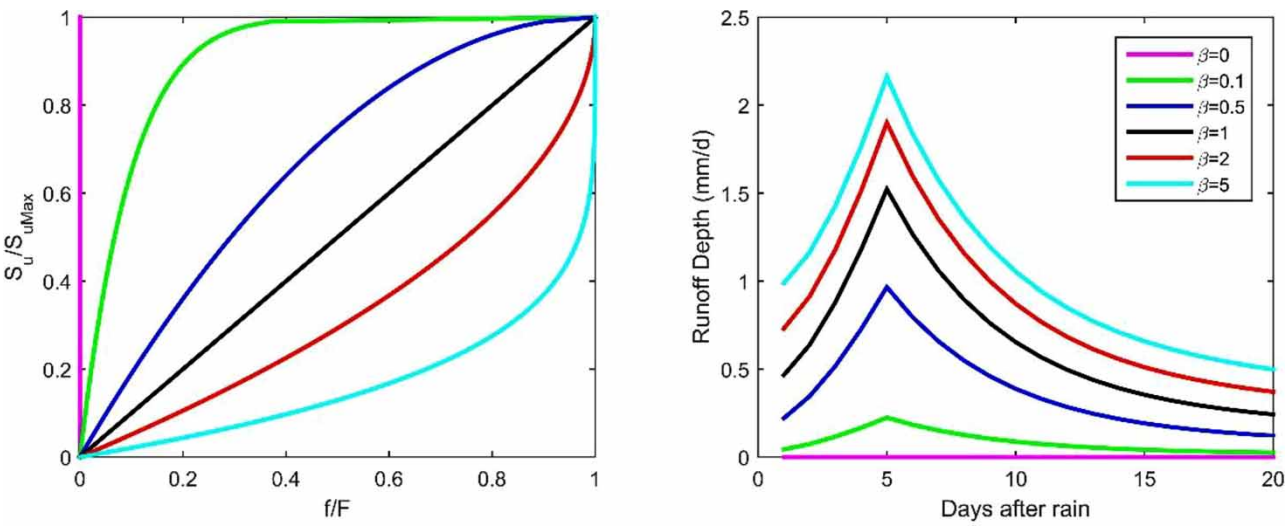

Figure 3 | The impact of different β values on streamflow generation. The left figure shows the impact on the shape of the Xinanjiang storage capacity curve, and the right figure shows the hydrograph generated by different β values. The amount of instantaneous precipitation is set as 20 mm. The initial condition of buckets and other parameters are kept constant. The S_{uMax} is set as 100 mm, with antecedent soil moisture (S_u) as 50 mm.

infiltrated and runoff generation is limited when soil moisture is low. In this case, flat peak flow is generated, as shown in the right panel of Figure 3. If β is larger than 1, the storage capacity curve will become a concave curve, which means the fraction of runoff to rainfall is much larger than the case of β with smaller values. In this condition, the shape of flood hydrograph will be higher, thinner and sharper (Figure 3). In summary, Figure 3 demonstrates that the β parameter significantly affects the runoff response to rainfall, including the flood volume and the flood peak flow. Therefore, we can use the β value, as a lumped parameter, to quantify the storm-flood response. More specifically, the catchments with higher β values are more likely to generate floods with larger flood volumes and sharper and thinner flood hydrographs, and vice versa.

Model evaluation and parameter optimization

Two objective functions were used to evaluate model performance, since multi-objectives model evaluation is more robust when quantifying model performance under different criteria. The Kling-Gupta efficiency (Gupta *et al.* 2009) (I_{KGE}) was used as an objective function for calibration and the criteria to evaluate model performance (Equation (20)).

$$I_{KGE} = 1 - \sqrt{(r-1)^2 + (\alpha-1)^2 + (\varepsilon-1)^2} \quad (20)$$

where r is the linear correlation coefficient between simulated and observed; α ($\alpha = \sigma_m/\sigma_o$) is a measure of relative variability in the simulated and observed values, σ_m is the standard deviation of simulated streamflow, σ_o is the standard deviation of observed streamflow; and ε is the ratio between the average value of simulated and observed data. The I_{KGL} function, which is the I_{KGE} of the logarithmic streamflow (Fenicia *et al.* 2007; Gao *et al.* 2014b), has been applied to evaluate the model performance, emphasizing evaluation of the quality of baseflow simulation.

A multi-objective parameter optimized algorithm (MOSCEM-UA) (Vrugt *et al.* 2003) was applied for calibration purposes. The parameter sets on the Pareto-frontier were assumed to be behavioral parameter sets and can equally represent model performance under certain criteria. Therefore, we used all the parameter sets on Pareto frontier in the calibration. The number of complexes in MOSCEM-UA was set as 10 reflecting the number of parameters, and the number of initial samples was set to 200 and a total number of 50,000 model iterations for all the catchment runs. Since the model structure has been validated in the USA (Berghuijs *et al.* 2014; Gao *et al.* 2014b) and internationally (Fenicia *et al.* 2008; Gharari *et al.* 2014; Gao *et al.* 2016; Zhao *et al.* 2016), only these parameters were calibrated and no further validation was implemented.

Correlation analysis between landscape features and calibrated β values

Linear correlation analysis was conducted to understand the association between the calibrated β parameter and catchment features. Associations were quantified by the correlation coefficient (r), and significance was evaluated by the significance test (indicated as p), to diagnose whether r is different from zeros.

RESULTS AND DISCUSSION

Model performance

Figure 4 shows a boxplot of two objective functions (I_{KGE} and I_{KGL}) to summarize the model performance. The boxplot shows that the median value (50% percentile) of the I_{KGE} of the 404 MOPEX catchments is 0.72. The maximum

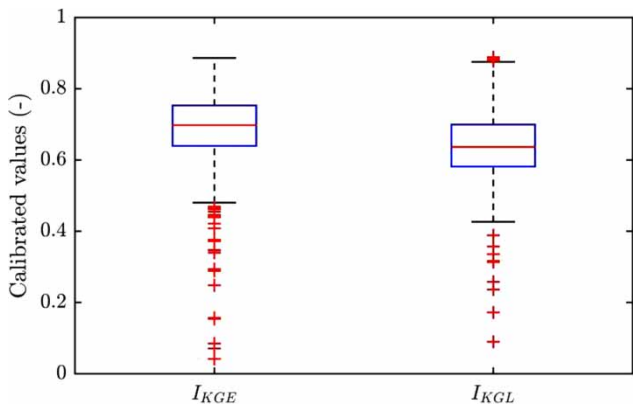

Figure 4 | Boxplots of the calibration performance of the FLEX model for all MOPEX catchments, with criteria of I_{KGE} and I_{KGL}.

and minimum values of the I_{KGE} whisker are 0.92 and 0.49, respectively. The 75% and 25% percentiles of the I_{KGE} boxplot are 0.78 and 0.63, respectively. For the boxplot of the I_{KGL}, the median value is 0.66, with 0.89 and 0.43 for the maximum and minimum of the whisker, respectively, and 0.71 and 0.59 for the 75% and 25% percentiles, respectively. The results show that the FLEX model can perform well to simulate the hydrological processes of most MOPEX catchments (Duan *et al.* 2006; Ye *et al.* 2014).

Figure 5 shows the spatial distribution patterns of the two objective functions. In relation to the spatial distribution of I_{KGE}, catchments in the east and west coast of the CONUS outperform simulations in the interior regions, most probably due to the impacts of the arid interior climate. This is in line with previous hydrological studies that more arid zones are characterized by poorer model performances (Wheater *et al.* 2007; Berghuijs *et al.* 2014). The model performance in relation to the I_{KGL} function is less clear. The I_{KGL} function is more sensitive to baseflow simulation, where human activities, including dams, irrigation and water allocation (Wang & Hejazi 2011), have more influence than natural processes.

The β values of the MOPEX catchments

The β value of each catchment was optimized and calibrated for each of the 404 MOPEX catchments and for each, the averaged β value on all Pareto-frontier parameter sets was regarded as the β of that catchment. In Figure 6, the β value of each catchment is shown together with the slope map. The β values exhibit a strong spatial distribution pattern in the 404 MOPEX catchments, and generally, the β parameter has a strong positive correlation with slope. Figure 6 clearly shows that the catchments with relatively small β values (0.01–0.5) have flat slopes, and these catchments are mostly located in Great Plain the interior region of the CONUS. This means the flatter catchments tend to generate relatively dampened flood peaks, as indicated by smaller β values. In contrast, the catchments located in the Rocky Mountains and the Appalachian Mountains have lager β values (>0.5). This indicates that catchments with steeper slopes have relatively high, sharp and thin flood peaks, which is in line with previous studies (Ruiz-Villanueva *et al.* 2010; Bodoque *et al.* 2015). The regionalized pattern of the β parameter can help us to understand and predict hydrological processes and flood peak flow in ungauged basins.

Correlations between landscape features and calibrated β values

Figure 7 shows the correlations between the calibrated β values and the catchment landscape features considered for all 404 catchments. Specifically, the β value increases with increases in the catchment averaged slope, elevation, impermeable area, and percentage of forest. These positive correlations can be interpreted from the perspective of catchment rainfall-runoff processes. Particularly, steeper slopes are prone to generate sharper (higher and thinner) flood peak flow represented as larger beta values, since steeper catchments have larger gravitational potential energy

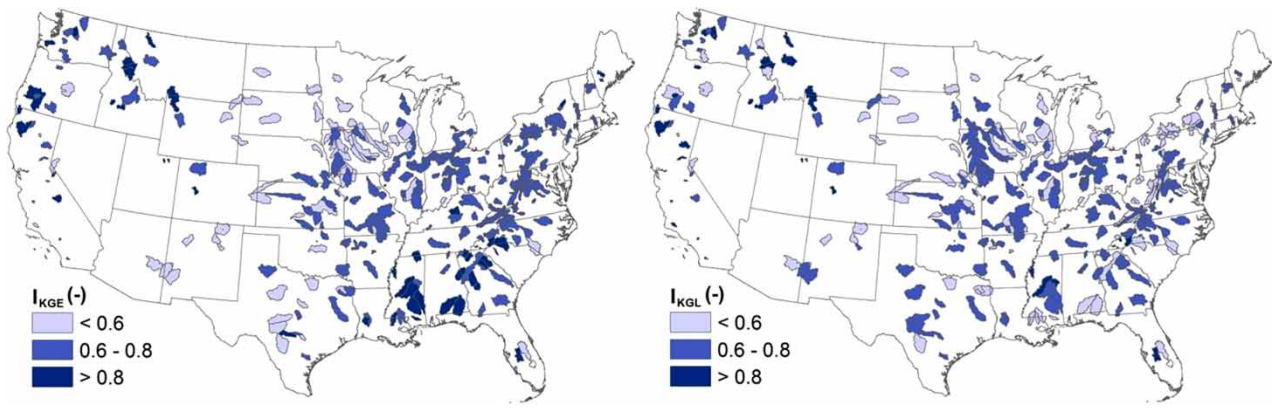

Figure 5 | The FLEX model calibration performance for each individual MOPEX catchment, with criteria of I_{KGE} and I_{KGL}.

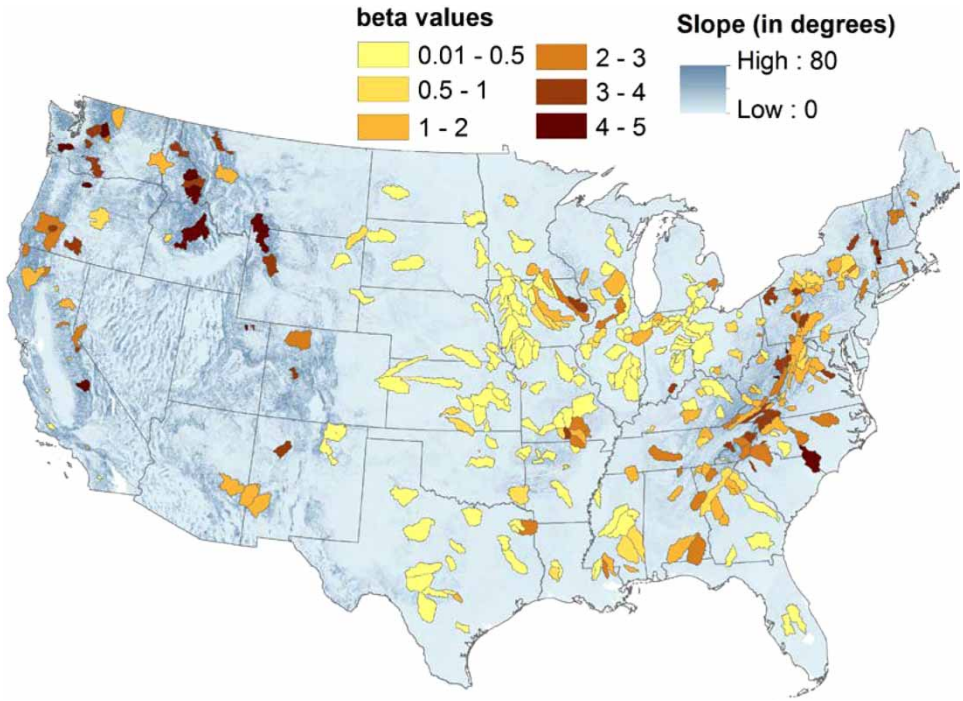

Figure 6 | The spatial distribution of β for the MOPEX catchments. The background map is the slope of the CONUS.

causing the quicker release of generated runoff and thus resulting in more concentrated flooding in a short time. Similar to the slope, elevation also has a positive correlation with β values, which is probably due to the fact that most areas with steep slopes are located in regions of higher elevation. Additionally, larger urban area corresponds with thinner and higher peak flow and larger β values, since the urbanized areas are normally characterized by impermeable surfaces (Grimm *et al.* 2008), reduced soil storage capacity and altered rainfall infiltration and surface runoff generation (Lee & Heaney 2003).

It is worth noting the positive correlation between forest proportion and beta values, which means a larger proportion of forest cover is associated with higher flood peak flow. The impact of forest cover on flood peak flow is still controversial in the hydrology community (Robinson *et al.* 2003; Andréassian 2004), because some studies have found that forest can reduce peak flow for small and medium floods (Sriwongsitanon & Taesombat 2011). Therefore, a negative correlation between β and forest cover was expected. We suggest three factors may be contributing to this positive correlation: (1) the spatial concurrence of mountainous region and forest cover, linked to a greater likelihood of anthropogenic activities such as deforestation and reclamation in flat areas. This may refer that the correlation of β and forest cover is due to the coherent of forest and mountainous region rather than forest cover itself; (2) the positive correlation between forest cover and precipitation, as Duan & Bastiaanssen (2013) found by satellite data; and (3) the complexity of simultaneously considering time and space. From a temporal perspective, deforestation likely increases flood peak flow, and reforestation probably decreases peak flow. In spatial terms, there are still few studies that address the association between flood peak flow and area proportion of forest cover with large sample dataset (Weingartner *et al.* 2003), and no clear relation has been found between forest proportion and flood discharge. Further research is therefore needed to explore the relation between forest cover and flood peak flow.

In contrast, the calibrated β parameter has a negative correlation with the soil erodibility factor (K factor), aridity index, the depth to bedrock and catchment area. Specifically, soils with a low K factor are very likely those with a higher proportion of clay and less detachment, which are prone to reduce infiltration and generate higher and sharper flood peak flows. The aridity index, representing climate,

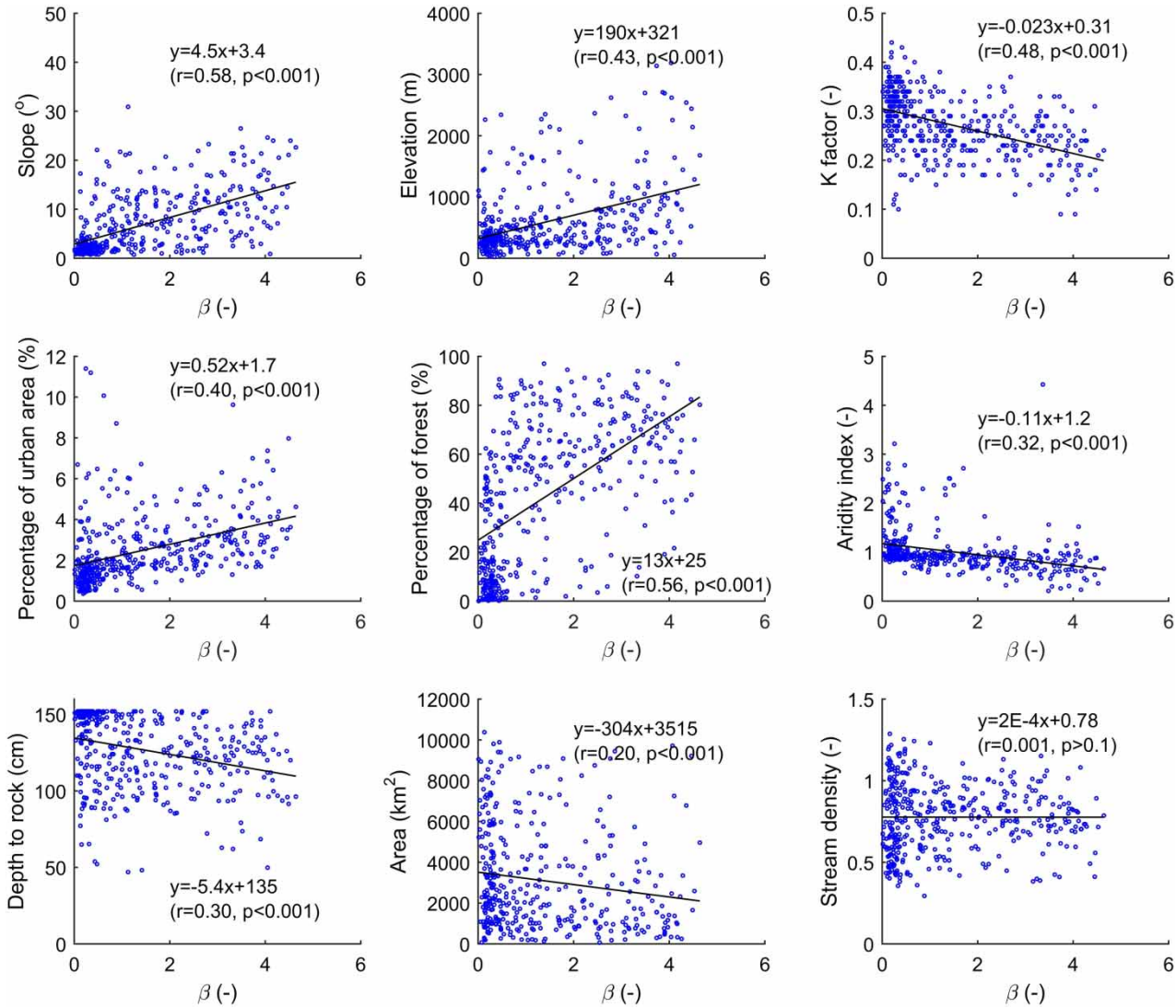

Figure 7 | Correlations between landscape features and β. Each blue dot indicates an individual catchment. r is the correlation coefficient, and p is the significance. Please refer to the online version of this paper to see this figure in colour: http://dx.doi.org.10.2166/nh.2017.245.

determines the correlation between precipitation and potential evaporation, water supply and evaporation demand. The negative correlation between aridity index and β indicates that in arid catchments soil is generally in an unsaturated condition, which allows more rainfall to infiltrate and thus reduces the peak flow and β values. The catchments with a shallower soil layer (the depth to bedrock) have less storage capacity, which makes them prone to flood generation. Catchment area also correlated negatively with β values, indicating that catchments with smaller area are apt to generate sharper flood peaks, probably due to the smaller capacity of channels in small catchments to regulate flood peaks. Catchments with larger areas generate flatter hydrographs than small catchments, because of the larger regulating capacity of the river channel network and the averaging effect of floods from different tributaries. This could also be related to there being a greater chance that rainfall is nonuniformly high across smaller catchments, and in larger catchments there is a greater chance for other processes to buffer the flood flows. The stream density had no significant correlation with β and the range of responses suggests that stream density can either increase flood peaks or reduce flood peaks depending on specific local geomorphology and channel bathymetry.

In summary, among all considered catchment features, slope has the largest impact on β and flood peaks, with a correlation coefficient (r) of 0.58 ($p < 0.001$) (Figure 7). The percentage of forest cover has the second largest impact on the β parameter, with r of 0.56 ($p < 0.001$). The K factor, elevation, impermeable area, aridity index, the depth to bedrock and catchment area also have significant impacts on β ($p < 0.001$), but with lower correlation coefficients (from 0.2 to 0.48) (Figure 7). Vegetation, soil characteristics, urban area, climate, geology and catchment area also impact flood peaks, but with weaker correlations. A clear spatial distribution pattern of the β parameter was also found. These conclusions are generally in line with previous parameter regionalization studies in Austria (Merz & Blöschl 2004) and the southeast of England (Wagener & Wheater 2006).

Implications and limitations

This research highlights the impact of topography on flood peaks. Globally, mountain flooding is an increasing risk to human populations, as settlement in these areas increases (Ruiz-Villanueva *et al.* 2010). Between 2000 and 2010, floods in mountain regions resulted in 1079 casualties every year in China, accounting for 65–92% of total flooding casualties. Mountain basins are often poorly gauged, and given the potential impacts of flash flooding in these areas, this study will be beneficial to predicting floods in mountainous regions. The findings of this study also have practical implications. For example, to reduce the peak flow for flood mitigation, we should take measures to reduce relative slope (e.g. building terraced fields), reduce the proportion of impermeable areas (using green roofs, permeable roads, green spaces and other ecosystems to absorb rainwater in urban areas), or increase the soil infiltration capacity (e.g. reforestation), For example, our results suggest that implementing the 'sponge city' in China could reduce flood impacts (Xia *et al.* 2017).

However, it should be noted that there are several limitations in our current study that should be addressed in further studies. Only nine catchment attributes were considered in this study, and further attributes should be explored in future research. In addition, for each of the considered features we used a single value (catchment-average) to represent each catchment in this study, and neither the variation nor the spatial distribution of corresponding features (e.g. distribution pattern of topography, vegetation and soil texture within catchments) were taken into account. How these spatial distribution patterns could be represented should be investigated further.

SUMMARY

In this study, we used the MOPEX dataset encompassing 404 catchments in the USA to explore the correlations between the shape parameter (β) of the storage capacity curve and various typical catchment features. We found that the β parameter, has clear regional patterns, influenced by topography, vegetation, soil, urban area, geology, and catchment area after controlling for the flood flows given rainfall and antecedent soil moisture. Generally, the catchments with steeper slopes, less erodible soil texture, larger impermeable areas, shallower soil depth, and smaller catchment areas will have larger β values, and thus are prone to sharper flood peaks. Among these features, topography has the largest impact on peak flow. This study is beneficial to understanding parameter regionalization related to flood peak flow and the impact of catchment features thereon.

ACKNOWLEDGEMENTS

This research is supported by the National Natural Science Foundation of China (Grant No. 91547202, 51479216), the State Key Laboratory of Cryospheric Sciences, Cold and Arid Regions Environment and Engineering Research Institute, Chinese Academy Sciences (SKLCS-OP-2016-04), and the Key Laboratory of Mountain Hazards and Earth Surface Process, Chinese Academy of Sciences (KLMHESP-17-02), and the National Key Research and Development Program of China (No. 2016YFC0402600). We thank Wouter Berghuijs for sharing the catchment characteristic information of the MOPEX catchments, and Dingbao Wang for generously sharing the shapefile of the MOPEX map. Thanks also go to Eric Moody for his review and grammatical corrections for the final manuscript. We would like to thank two anonymous

reviewers and editor Nevil Wyndham Quinn for their valuable and constructive comments and suggestions for improving this manuscript.

REFERENCES

Andréassian, V. 2004 Waters and forests: from historical controversy to scientific debate. *Journal of Hydrology* **291**, 1–27. http://dx.doi.org/10.1016/j.jhydrol.2003.12.015.

Austin, A. T., Yahdjian, L., Stark, J. M., Belnap, J., Porporato, A., Norton, U., Ravetta, D. A. & Schaeffer, S. M. 2004 Water pulses and biogeochemical cycles in arid and semiarid ecosystems. *Oecologia* **141**, 221–235. DOI: 10.1007/s00442-004-1519-1.

Berghuijs, W. R., Sivapalan, M., Woods, R. A. & Savenije, H. H. G. 2014 Patterns of similarity of seasonal water balances: a window into streamflow variability over a range of time scales. *Water Resources Research* **50**, 5638–5661. DOI: 10.1002/2014WR015692.

Berghuijs, W. R., Woods, R. A., Hutton, C. J. & Sivapalan, M. 2016 Dominant flood generating mechanisms across the United States. *Geophysical Research Letters* **43**, 4382–4390. DOI: 10.1002/2016GL068070.

Bergström, S. & Forsman, A. 1973 Development of a conceptual deterministic rainfall-runoff model. *Nordic Hydrology* **4**, 147–170.

Bergström, S. & Lindström, G. 2015 Interpretation of runoff processes in hydrological modelling – experience from the HBV approach. *Hydrological Processes* **29**, 3535–3545.

Beven, K. 2004a Robert E. Horton's perceptual model of infiltration processes. *Hydrological Processes* **18**, 3447–3460. DOI: 10.1002/hyp.5740.

Beven, K. 2004b Robert E. Horton and abrupt rises of ground water. *Hydrological Processes* **18**, 3687–3696. DOI: 10.1002/hyp.5741.

Beven, K. J. 2012 *Rainfall–Runoff Models: The Primer*. John Wiley & Co., London.

Beven, K. & Freer, J. 2001 A dynamic topmodel. *Hydrological Processes* **15**, 1993–2011. DOI: 10.1002/hyp.252.

Beven, K. J. & Kirkby, M. J. 1979 A physically based, variable contributing area model of basin hydrology. *Hydrological Sciences Bulletin* **24**, 43–69. DOI: 10.1080/02626667909491834.

Blaikie, P., Cannon, T., Davis, I. & Wisner, B. 2014 *At Risk: Natural Hazards, People's Vulnerability and Disasters*. Routledge, Abingdon, UK.

Blöschl, G., Ardoin-Bardin, S., Bonell, M., Dorninger, M., Goodrich, D., Gutknecht, D., Matamoros, D., Merz, B., Shand, P. & Szolgay, J. 2007 At what scales do climate variability and land cover change impact on flooding and low flows? *Hydrological Processes* **21** (9), 1241–1247. DOI: 10.1002/hyp.6669.

Blöschl, G., Gaál, L., Hall, J., Kiss, A., Komma, J., Nester, T., Parajka, J., Perdigão, R. A. P., Plavcová, L., Rogger, M., Salinas, J. L. & Viglione, A. 2015 Increasing river floods: fiction or reality? *Wiley Interdisciplinary Reviews: Water* **2**, 329–344. DOI: 10.1002/wat2.1079.

Bodoque, J. M., Díez-Herrero, A., Eguibar, M. A., Benito, G., Ruiz-Villanueva, V. & Ballesteros-Cánovas, J. A. 2015 Challenges in paleoflood hydrology applied to risk analysis in mountainous watersheds – a review. *Journal of Hydrology* **529** (Part 2), 449–467. http://dx.doi.org/10.1016/j.jhydrol.2014.12.004

Brooks, R. J., Barnard, H. R., Coulombe, R. & McDonnell, J. J. 2010 Ecohydrologic separation of water between trees and streams in a Mediterranean climate. *Nature Geoscience* **3**, 100–104. DOI: 10.1038/ngeo722.

Budyko, M. I. 1974 *Climate and Life*. Academic Press/Elsevier, The Netherlands.

Burt, T. P. & McDonnell, J. J. 2015 Whither field hydrology? The need for discovery science and outrageous hydrological hypotheses. *Water Resources Research* **51**, 5919–5928. DOI: 10.1002/2014WR016839.

Dai, Y., Zeng, X., Dickinson, R. E., Baker, I., Bonan, G. B., Bosilovich, M. G., Denning, A. S., Dirmeyer, P. A., Houser, P. R., Niu, G., Oleson, K. W., Schlosser, C. A. & Yang, Z.-L. 2003 The common land model. *Bulletin of the American Meteorological Society* **84**, 1013–1023. DOI: 10.1175/BAMS-84-8-1013.

De Groen, M. M. & Savenije, H. H. G. 2006 A monthly interception equation based on the statistical characteristics of daily rainfall. *Water Resources Research* **42**. DOI: 10.1029/2006WR005013.

DHI 2012 *Thailand Floods 2011 – The Need for Holistic Flood Risk Management*. DHI-NTU Research Centre, Singapore.

Duan, Z. & Bastiaanssen, W. G. M. 2013 First results from Version 7 TRMM 3b43 precipitation product in combination with a new downscaling–calibration procedure. *Remote Sensing of the Environment* **131**, 1–13. DOI: 10.1016/j.rse.2012.12.002.

Duan, Q., Schaake, J., Andréassian, V., Franks, S., Goteti, G., Gupta, H. V., Gusev, Y. M., Habets, F., Hall, A., Hay, L., Hogue, T., Huang, M., Leavesley, G., Liang, X., Nasonova, O. N., Noilhan, J., Oudin, L., Sorooshian, S., Wagener, T. & Wood, E. F. 2006 Model Parameter Estimation Experiment (MOPEX): an overview of science strategy and major results from the second and third workshops. *Journal of Hydrology* **320**, 3–17. DOI: 10.1016/j.jhydrol.2005.07.031.

Dunne, T. & Black, R. D. 1970 Partial area contributions to storm runoff in a small New England Watershed. *Water Resources Research* **6**, 1296–1311. DOI: 10.1029/WR006i005p01296.

Fenicia, F., Savenije, H. H. G., Matgen, P. & Pfister, L. 2007 A comparison of alternative multiobjective calibration strategies for hydrological modeling. *Water Resources Research* **43**. DOI: 10.1029/2006WR005098.

Fenicia, F., Savenije, H. H. G., Matgen, P. & Pfister, L. 2008 Understanding catchment behavior through stepwise model concept improvement. *Water Resources Research* **44**, 1–13. DOI: 10.1029/2006WR005563.

Fenicia, F., Kavetski, D. & Savenije, H. H. G. 2011 Elements of a flexible approach for conceptual hydrological modeling: 1. Motivation and theoretical development. *Water Resources Research* **47**. DOI: 10.1029/2010WR010174.

Fu, B. P. 1981 On the calculation of the evaporation from land surface. *Sci. Atmos. Sin.* **5**, 23–31 (In Chinese).

Gao, H., He, X., Ye, B. & Pu, J. 2012 Modeling the runoff and glacier mass balance in a small watershed on the Central Tibetan Plateau, China, from 1955 to 2008. *Hydrological Processes* **26**, 1593–1603. DOI: 10.1002/hyp.8256.

Gao, H., Hrachowitz, M., Fenicia, F., Gharari, S. & Savenije, H. H. G. 2014a Testing the realism of a topography-driven model (FLEX-Topo) in the nested catchments of the Upper Heihe, China. *Hydrology and Earth System Sciences* **18**, 1895–1915. DOI: 10.5194/hess-18-1895-2014.

Gao, H., Hrachowitz, M., Schymanski, S. J., Fenicia, F., Sriwongsitanon, N. & Savenije, H. H. G. 2014b Climate controls how ecosystems size the root zone storage capacity at catchment scale. *Geophysical Research Letters* **41**, 7916–7923. DOI: 10.1002/2014GL061668.

Gao, H., Hrachowitz, M., Sriwongsitanon, N., Fenicia, F., Gharari, S. & Savenije, H. H. G. 2016 Accounting for the influence of vegetation and landscape improves model transferability in a tropical savannah region. *Water Resources Research* **52**, 7999–8022.

Gao, H., Han, T., Liu, Y. & Zhao, Q. 2017 Use of auxiliary data of topography, snow and ice to improve model performance in a glacier dominated catchment in Central Asia. *Hydrology Research* **48** (5), 1418–1437. DOI: 10.2166/nh.2016.242.

Gharari, S., Hrachowitz, M., Fenicia, F., Gao, H. & Savenije, H. H. G. 2014 Using expert knowledge to increase realism in environmental system models can dramatically reduce the need for calibration. *Hydrology and Earth System Sciences* **18**, 4839–4859. DOI: 10.5194/hess-18-4839-2014.

Grimm, N. B., Faeth, S. H., Golubiewski, N. E., Redman, C. L., Wu, J., Bai, X. & Briggs, J. M. 2008 Global change and the ecology of cities. *Science* **319**, 756–760. DOI: 10.1126/science.1150195.

Gupta, H. V., Kling, H., Yilmaz, K. K. & Martinez, G. F. 2009 Decomposition of the mean squared error and NSE performance criteria: implications for improving hydrological modelling. *Journal of Hydrology* **377**, 80–91. DOI: 10.1016/j.jhydrol.2009.08.003.

Gupta, H. V., Perrin, C., Blöschl, G., Montanari, A., Kumar, R., Clark, M. & Andréassian, V. 2014 Large-sample hydrology: a need to balance depth with breadth. *Hydrology and Earth System Sciences* **18**, 463–477. DOI: 10.5194/hess-18-463-2014.

Hargreaves, G. H. & Samani, Z. A. 1985 Reference crop evapotranspiration from temperature. *Applied Engineering in Agriculture* **1**, 96–99.

Hewlett, J. D. 1961 *Soil Moisture as a Source of Base Flow From Steep Mountain Watersheds.* Southeastern Forest Experiment Station, US Department of Agriculture, Forest Service, Asheville, NC, USA.

Hewlett, J. D. & Troendle, C. A. 1975 Non-point and diffused water sources: a variable source area problem. In: *Symposium on Watershed Management*. American Society of Civil Engineers, VA, pp. 21–46.

Hirabayashi, Y., Mahendran, R., Koirala, S., Konoshima, L., Yamazaki, D., Watanabe, S., Kim, H. & Kanae, S. 2013 Global flood risk under climate change. *Nature Climate Change* **3**, 816–821. DOI: 10.1038/nclimate1911.

Hock, R. 2003 Temperature index melt modelling in mountain areas. *Journal of Hydrology* **282**, 104–115. DOI: 10.1016/S0022-1694(03)00257-9.

Homer, C. G., Dewitz, J. A., Yang, L., Jin, S., Danielson, P., Xian, G., Coulston, J., Herold, N. D., Wickham, J. D. & Megown, K. 2015 Completion of the 2011 National Land Cover Database for the conterminous United States-representing a decade of land cover change information. *Photogrammetric Engineering and Remote Sensing* **81**, 345–354.

Horton, R. E. 1933 The role of infiltration in the hydrologic cycle. *Transactions, American Geophysical Union* **14**, 446–460.

Hrachowitz, M., Savenije, H. H. G., Blöschl, G., McDonnell, J. J., Sivapalan, M., Pomeroy, J. W., Arheimer, B., Blume, T., Clark, M. P., Ehret, U., Fenicia, F., Freer, J.E., Gelfan, A., Gupta, H. V., Hughes, D. A., Hut, R. W., Montanari, A., Pande, S., Tetzlaff, D., Troch, P. A., Uhlenbrook, S., Wagener, T., Winsemius, H. C., Woods, R.A., Zehe, E. & Cudennec, C. 2013 A decade of predictions in ungauged basins (PUB) – a review. *Hydrological Sciences Journal* **58**, (6) 1198–1255. DOI: 10.1080/02626667.2013.803183.

Jasechko, S., Sharp, Z. D., Gibson, J. J., Birks, S. J., Yi, Y. & Fawcett, P. J. 2013 Terrestrial water fluxes dominated by transpiration. *Nature* **496**, (7445) 347–350. DOI: 10.1038/nature11983.

Kling, H. & Gupta, H. 2009 On the development of regionalization relationships for lumped watershed models: the impact of ignoring sub-basin scale variability. *Journal of Hydrology* **373**, 337–351. DOI: 10.1016/j.jhydrol.2009.04.031.

Lee, J. G. & Heaney, J. P. 2003 Estimation of urban imperviousness and its impacts on storm water systems. *Journal of Water Resources Planning and Management* **129**, 419–426.

Li, Z., Huang, P., Yao, C., Li, Q., Zhao, L. & Yu, Z. 2014 Application of flexible-structure hydrological models in different runoff generation regions. *Advances in Water Sciences* **25**, 28–35.

Liang, X., Lettenmaier, D. P., Wood, E. F. & Burges, S. J. 1994 A simple hydrologically based model of land surface water and energy fluxes for general circulation models. *Journal of Geophysical Research* **99** (D7), 14415. DOI: 10.1029/94JD00483.

Liu, D., Tian, F., Hu, H. & Hu, H. 2012 The role of run-on for overland flow and the characteristics of runoff generation in the Loess Plateau, China. *Hydrological Sciences Journal* **57**, 1107–1117. DOI: 10.1080/02626667.2012.695870.

Merz, R. & Blöschl, G. 2004 Regionalisation of catchment model parameters. *Journal of Hydrology* **287**, 95–123. DOI: 10.1016/j.jhydrol.2003.09.028.

Milly, P. C. D., Betancourt, J., Falkenmark, M., Hirsch, R. M., Kundzewicz, Z. W., Lettenmaier, D. P. & Stouffer, R. J. 2008 Stationarity is dead: whither water management? *Science* **319** (5863), 573–574. DOI: 10.1126/science.1151915.

Mo, W. & Zhang, Q. 2013 Energy–nutrients–water nexus: integrated resource recovery in municipal wastewater treatment plants. *Journal of Environmental Management* **127**, 255–267. http://dx.doi.org/10.1016/j.jenvman.2013.05.007

Montanari, A., Young, G., Savenije, H. H. G., Hughes, D., Wagener, T., Ren, L. L., Koutsoyiannis, D., Cudennec, C., Toth, E., Grimaldi, S., Blöschl, G., Sivapalan, M., Beven, K., Gupta, H., Hipsey, M., Schaefli, B., Arheimer, B., Boegh, E., Schymanski, S. J., Di Baldassarre, G., Yu, B., Hubert, P., Huang, Y., Schumann, A., Post, D. A., Srinivasan, V., Harman, C., Thompson, S., Rogger, M., Viglione, A., McMillan, H., Characklis, G., Pang, Z. & Belyaev, V. 2013 'Panta Rhei – everything flows': change in hydrology and society – the IAHS scientific decade 2013–2022. *Hydrological Sciences Journal* **58**, 1256–1275. DOI: 10.1080/02626667.2013.809088.

Moore, R. J. 2007 The PDM rainfall-runoff model. *Hydrology and Earth System Sciences Discussions* **11**, 483–499.

Palmer, M. A., Liu, J., Matthews, J. H., Mumba, M. & D'Odorico, P. 2015 Manage water in a green way. *Science* **349**, 584–585.

Peel, M. C., Chiew, F. H. S., Western, A. W. & McMahon, T. A. 2000 *Extension of Unimpaired Monthly Streamflow Data and Regionalisation of Parameter Values to Estimate Streamflow in Ungauged Catchments, National Land and Water Resources Audit, Theme 1 – Water Availability.* Centre for Environmental Applied Hydrology, The University of Melbourne, Melbourne, p. 37.

Perrin, C., Michel, C. & Andréassian, V. 2001 Does a large number of parameters enhance model performance? Comparative assessment of common catchment model structures on 429 catchments. *Journal of Hydrology* **242**, 275–301. DOI: 10.1016/S0022-1694(00)00393-0.

Renard, K. G., Yoder, D. C., Lightle, D. T. & Dabney, S. M. 2011 Universal soil loss equation and revised universal soil loss equation. *Handbook of Erosion Modelling* **8**, 135–167.

Robinson, M., Cognard-Plancq, A.-L., Cosandey, C., David, J., Durand, P., Führer, H.-W., Hall, R., Hendriques, M. O., Marc, V., McCarthy, R., McDonnell, M., Martin, C., Nisbet, T., O'Dea, P., Rodgers, M. & Zollner, A. 2003 Studies of the impact of forests on peak flows and baseflows: a European perspective. *Forest Ecology and Management* **186**, 85–97. http://dx.doi.org/10.1016/S0378-1127(03)00238-X

Ruiz-Villanueva, V., Díez-Herrero, A., Stoffel, M., Bollschweiler, M., Bodoque, J. M. & Ballesteros, J. A. 2010 Dendrogeomorphic analysis of flash floods in a small ungauged mountain catchment (Central Spain). *Geomorphology* **118**, 383–392. http://dx.doi.org/10.1016/j.geomorph.2010.02.006

Samaniego, L., Kumar, R. & Attinger, S. 2010 Multiscale parameter regionalization of a grid-based hydrologic model at the mesoscale. *Water Resources Research* **46**. DOI: 10.1029/2008WR007327.

Schwarz, G. E. & Alexander, R. B. 1995 *State Soil Geographic (STATSGO) Data Base for the Conterminous United States*. Open File report 95-449, US Geological Survey, Washington, DC.

Sellers, P. J., Los, S. O., Tucker, C. J., Justice, C. O., Dazlich, D. A., Collatz, G. J. & Randall, D. A. 1996 A revised land surface parameterization (sib2) for atmospheric GCMs. Part II: the generation of global fields of terrestrial biophysical parameters from satellite data. *Journal of Climate* **9**, 706–737. DOI: 10.1175/1520-0442(1996)009 < 0706:ARLSPF > 2.0.CO;2.

Singh, V. P. & Woolhiser, D. A. 2002 Mathematical modeling of watershed hydrology. *Journal of Hydrologic Engineering* **7**, 270–292. DOI: 10.1061/(ASCE)1084-0699(2002)7:4(270).

Sivapalan, M. & Woods, R. A. 1995 Evaluation of the effects of general circulation models' subgrid variability and patchiness of rainfall and soil moisture on land surface water balance fluxes. *Hydrological Processes* **9**, 697–717.

Sivapalan, M., Takeuchi, K., Franks, S. W., Gupta, V. K., Karambiri, H., Lakshmi, V., Liang, X., McDonnell, J. J., Mendiondo, E. M., O'Connell, P. E., Oki, T., Pomeroy, J. W., Schertzer, D., Uhlenbrook, S. & Zehe, E. 2003 IAHS decade on Predictions in Ungauged Basins (PUB), 2003–2012: shaping an exciting future for the hydrological sciences. *Hydrological Sciences Journal* **48**, 857–880. DOI: 10.1623/hysj.48.6.857.51421.

Sklash, M. G. & Farvolden, R. N. 1979 The role of groundwater in storm runoff. *Journal of Hydrology* **43** (1), 45–65. DOI: http://dx.doi.org/10.1016/0022-1694(79)90164-1.

Sriwongsitanon, N. & Taesombat, W. 2011 Effects of land cover on runoff coefficient. *Journal of Hydrology* **410**, 226–238. DOI: 10.1016/j.jhydrol.2011.09.021.

Stonestrom, D. A., Scanlon, B. R. & Zhang, L. 2009 Introduction to special section on impacts of land use change on water resources. *Water Resources Research* **45**. DOI: 10.1029/2009WR007937.

Todini, E. 1996 The ARNO rainfall–runoff model. *Journal of Hydrology* **175**, 339–382. http://dx.doi.org/10.1016/S0022-1694(96)80016-3

Tromp-van Meerveld, H. J. & McDonnell, J. J. 2006 Threshold relations in subsurface stormflow: 1. A 147-storm analysis of the Panola hillslope. *Water Resources Research* **42**. DOI: 10.1029/2004WR003778.

Vrugt, J. A., Gupta, H. V., Bastidas, L. A., Bouten, W. & Sorooshian, S. 2003 Effective and efficient algorithm for multiobjective optimization of hydrologic models. *Water Resources Research* **39**, 1–19. DOI: 10.1029/2002WR001746.

Wagener, T. & Wheater, H. S. 2006 Parameter estimation and regionalization for continuous rainfall-runoff models including uncertainty. *Journal of Hydrology* **320**, 132–154.

Wang, D. & Hejazi, M. 2011 Quantifying the relative contribution of the climate and direct human impacts on mean annual streamflow in the contiguous United States. *Water Resources Research* **47**. DOI: 10.1029/2010WR010283.

Weingartner, R., Barben, M. & Spreafico, M. 2003 Floods in mountain areas – an overview based on examples from Switzerland. *Journal of Hydrology* **282**, 10–24.

Wheater, H., Sorooshian, S. & Sharma, K. D. 2007 *Hydrological Modelling in Arid and Semi-Arid Areas.* Cambridge University Press, Cambridge, UK.

Winsemius, H. C., Aerts, J. C. J. H., van Beek, L. P. H., Bierkens, M. F. P., Bouwman, A., Jongman, B., Kwadijk, J. C. J., Ligtvoet, W., Lucas, P. L. & van Vuuren, D. P. 2016 Global drivers of future river flood risk. *Nature Climate Change* **6**, 381–385.

Wolock, D. M. 1997 *STATSGO Soil Characteristics for the Conterminous United States.* US Geological Survey, Washington, DC.

Wood, E. F., Lettenmaier, D. P. & Zartarian, V. G. 1992 A land-surface hydrology parameterization with subgrid variability for general circulation models. *Journal of Geophysical Research* **97**, 2717. DOI: 10.1029/91JD01786.

Xia, J., Shi, W., Wang, Q. & Zou, L. 2017 Discussion of several hydrological issues regarding sponge city construction. *Water Resources Protection* **33**, 1–8. DOI: 10.3880/j.issn.1004 6933. 2017.01.001.

Xu, C.-Y. & Singh, P. V. 2004 Review on regional water resources assessment models under stationary and changing climate. *Water Resources Management* **18**, 591–612. DOI: 10.1007/s11269-004-9130-0.

Xu, C.-Y., Widén, E. & Halldin, S. 2005 Modelling hydrological consequences of climate change – progress and challenges. *Advances in Atmospheric Sciences* **22**, 789–797. DOI: 10.1007/BF02918679.

Ye, A., Duan, Q., Yuan, X., Wood, E. F. & Schaake, J. 2014 Hydrologic post-processing of MOPEX streamflow simulations. *Journal of Hydrology* **508**, 147–156.

Yu, Z., Lakhtakia, M. N. & Barron, E. J. 1999 Modeling the river basin response to single storm events simulated by a mesoscale meteorological model at various resolutions. *Journal of Geophysical Research* **104**, 19675–19690.

Yu, Z., Barron, E. J. & Schwartz, F. W. 2000 Retrospective simulation of a storm event: a first step in coupled climate/hydrologic modeling. *Geophysical Research Letter* **27**, 2561–2565.

Zhao, R.-J. 1992 The Xinanjiang model applied in China. *Journal of Hydrology* **135**, 371–381. DOI: 10.1016/0022-1694(92)90096-E.

Zhao, R.-J., Zuang, Y., Fang, L., Liu, X. & Zhang, Q. 1980 The Xinanjiang model. *Hydrological Forecasting – Prévisions Hydrologiques* **129**, 351–356.

Zhao, J., Xu, Z. & Singh, V. P. 2016 Estimation of root zone storage capacity at the catchment scale using improved Mass Curve Technique. *Journal of Hydrology* **540**, 959–972. http://dx.doi.org/10.1016/j.jhydrol.2016.07.013

First received 4 October 2016; accepted in revised form 6 May 2017. Available online 11 August 2017